Thin-Film Photovoltaics Partnership Program

Third Quarterly Status Report – Year III

Covering the period of April 2, 2004 to July 1, 2004

Deliverable:

Subcontract Article 3 B, **Item 17 Deliverable D.3.4 (**ADJ-2-30630-13**)**

Project: **Fundamental Materials Research and Advanced Process Development for Thin-Film CIS-Based Photovoltaics**

P.I.: T. J. Anderson

Co-PI's: Sheng S. Li, O.D. Crisalle, and Valentin Craciun

Other Personnel Ryan Acher, Ryan M. Kaczynski, Woo Kyoung Kim, Wei Liu, Josh Mangum, Matt Monroe, Zivin Park, Jiyon Song, Xuege Wang, and Seokhyun Yoon

Subcontract No.: ADJ-2-30630-13

Funding Agency: National Renewal Energy Laboratory (NREL)

Program: Thin-Film Photovoltaics Partnership program

Contact Address: Tim Anderson, P.O. Box 116005, 227 Chemical Engineering Bldg., University of Florida, Gainesville FL 32611-6005, Phone: (352) 392-0882, FAX: (352) 392-9513, E-mail: tim@nersp.nerdc.ufl.edu

1 Progress on Reaction Pathways and Kinetics of $CuInSe_2$ Formation from Selenization of Cu-In/Mo/glass Precursor.

Participants: Timothy J. Anderson and Oscar D. Crisalle (Faculty Advisors), Woo Kyoung Kim, Seokhyun Yoon, Ryan Acher, and Ryan Kaczynski (Graduate Research Assistants).

1.1 Objective

In-situ study of the reaction pathways and kinetics of $CuInSe_2$ formation from selenization of Cu-In/Mo/glass precursor using the time-resolved, high temperature X-ray diffraction.

1.2 Accomplishments during the current quarter

1.2.1 Preparation of precursor films

The Cu-In/Mo/glass and Cu-In/glass precursors were prepared using the PMEE (Plasma-assisted Migration Enhanced Epitaxy) reactor. During the deposition of elemental copper and indium, the substrates were not heated to minimize the possible reaction between copper and indium. The atomic composition ([Cu]/[Ga]~1.0) of as-grown precursor was determined by ICP.

1.3 Activities envisioned for the next quarter

The selenium (Se) chamber which can provide Se overpressure for high temperature XRD system using Se powder will be designed. In order to investigate the phase evolution during the selenization of Cu-In/Mo/glass precursor, the high temperature XRD system equipped with a Se chamber will be used.

2 Investigation of Pulsed Laser Annealing (PLA) of CIGS-Based Solar Cells

Participants: Xuege Wang, Sheng S. Li (Faculty Advisor), Seokhyun Yoon, V. Cracium, O. D. Crisalle, T. J. Anderson and J. Venturini

2.1 Objectives

The objective of this project is to study the effect of Laser Annealing (PLA) on the electrical and optical properties of CIS/CIGS based solar cells, and to find the optimal laser annealing condition for improving the cell's performance.

2.2 Accomplishments during the current quarter

The effects of PLA treatment on the film properties and the performance of CIGS solar cells have been studied by us under various annealing conditions [1]. Several characterization techniques have been used to study the effect of PLA treatment on the film properties and the performance of CIGS cells. The results show that PLA treatment under optimal laser energy density and pulse number has significant beneficial effects on the effective carrier lifetime, mobility, surface morphology, spectral response, diode quality factor and cell performance. The energy density of the laser beam and the number of pulse cycle were found to play a key role in modifying the optical and electrical properties of the CIGS films and hence the cell performance.

To study the laser annealing effect on film surface morphology, 5 identical CdS/CIGS films were annealed using a 250 ns pulsed 308 nm laser beam at selected laser energy density in the range 30 to 110 mJ/cm^2, 5 pulses. As illustrated by SEM micrographs shown in Figure 2-1, the surface morphology and apparent grain size increased upon laser annealing with energy density of 70 mJ/cm^2 or higher. This result suggests that the selected energy densities were sufficient to cause atomic rearrangement in the near surface region, and thus the potential exists to modify the atomic defects in the near surface region. More detailed SEM images with magnification of 40000x shown in Figure 2-2 suggest near surface morphology changes if we keep increasing the energy density of the laser beam. As one can see in Figure 2-2 d, e and f, the surface morphology changes dramatically when energy density of PLA is around 70 mJ/cm^2 or higher.

2.3 Activities envisioned for the next quarter

Our future efforts will be focused on the detailed study of PLA effect on modifying film surface structure by using XRD and XPS measurements. Also the effect of Rapid thermal annealing (RTA) treatments on CIGS absorbers and cell performance under different annealing conditions will be studied for the next quarter.

2.4 Publications and presentations

1. Xuege Wang, Sheng S. Li, C. H. Huang, Lei Li Kerr, S. Rawal, J. M. Howard, V. Craciun, T. J. Anderson, and O. D. Crisalle, "*Investigation of Pulsed Non-Melt Laser Annealing on the Film Properties and Performance of Cu(In,Ga)Se2 Solar Cells*", accepted, "Solar Energy Materials and Solar Cells"(2004).

2.5 References cited

[1] Xuege Wang, Sheng S. Li, C. H. Huang, Lei Li Kerr, S. Rawal, J. M. Howard, V. Craciun, T. J. Anderson, and O. D. Crisalle, "*Investigation of Pulsed Non-Melt Laser Annealing on the Film Properties and Performance of Cu(In,Ga)Se2 Solar Cells*", accepted,

"Solar Energy Materials and Solar Cells"(2004).

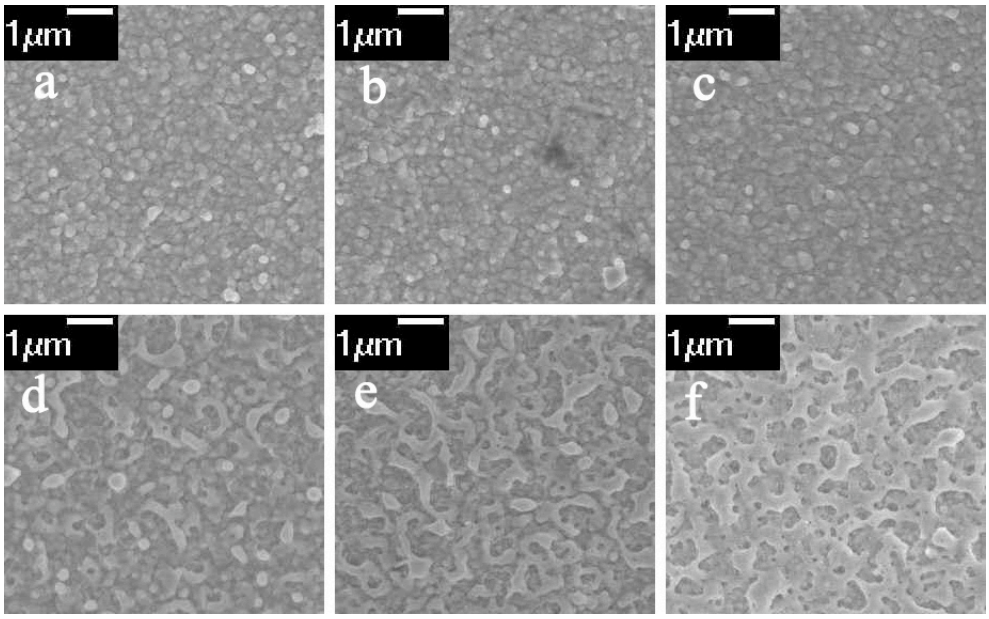

Figure 2-1 Surface morphology of CdS/CIGS films (a) before and after PLA treatment with energy densities at (b) 30 mJ/cm^2, (c) 50 mJ/cm^2, (d) 70 mJ/cm^2, (e) 90 mJ/cm^2, (f) 110 mJ/cm^2. (SEM images with magnification of 4000x).

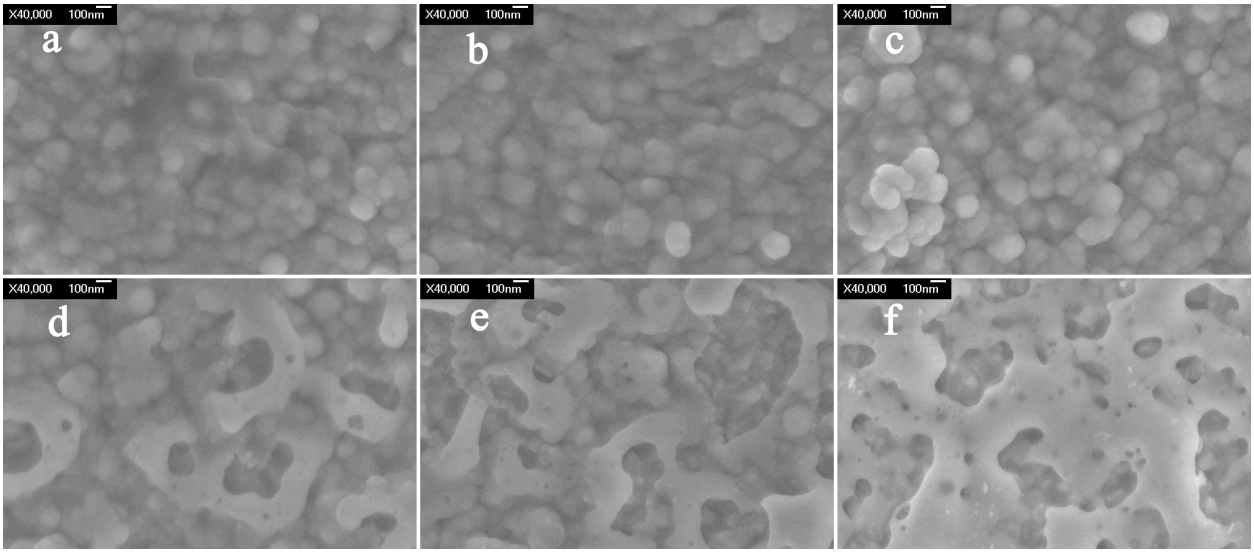

Figure 2-2 Surface morphology of CdS/CIGS films (a) before and after PLA treatment with energy densities at (b) 30 mJ/cm^2, (c) 50 mJ/cm^2, (d) 70 mJ/cm^2, (e) 90 mJ/cm^2, (f) 110 mJ/cm^2. (SEM images with magnification of 40000x).

3 Progress on Growth of $Cu(In,Ga)Se_2$ Absorber Films

Participants: Timothy J. Anderson, Oscar D. Crisalle, and Sheng S. Li (Faculty Advisors), and Ryan Kaczynski, Ryan Acher, Woo Kyoung Kim, Seokhyun Yoon (Graduate Research Assistants).

3.1 Objectives

Growth and characterization of $Cu(In,Ga)Se_2$ absorber layers.

3.2 Accomplishments during the current quarter

The growth of CIGS absorber films to study alternative buffer layers has been delayed. Approximately ten growth runs were completed before the gallium source started to malfunction. Three Mo-coated soda lime glass and one bare soda lime glass substrate were loaded into the plasma-assisted migration enhanced epitaxy (PMEE) reactor during each run. The rotation rate of the substrate platen was set to 12 rpm throughout the entire growth process. Overall compositions of the films were measured using the inductively coupled plasma (ICP) technique. The [Ga]/([In]+[Ga]) ratio was varied from 0 (CIS) to 1 (CGS) with special attention being paid to absorber films grown with a [Ga]/[In] ratio of approximately 0.3. The absorber thickness was also varied from 1 _m to 2 _m**.** The growth runs that have been completed used a constant flux process. The ratio [Cu]/([In]+[Ga]) remains relatively constant throughout the growth process while the growth temperature will be ~491°C (our maximum substrate temperature).

3.3 Activities envisioned for the next quarter

The first objective for the next quarter will be to repair the gallium source and to clean the reactor of the excess selenium that has been deposited over time. After the reactor has been repaired, NREL's 3-layer process will be incorporated into the PMEE reactor to grow CIGS. In+Ga+Se will be deposited during the first stage at approximately 400°C, and then Cu and Se will be added at ~491°C until the overall film composition becomes copper-rich. The composition will be returned to Cu-deficient by adding more In+Ga+Se until the desired overall composition is reached. XRD analysis and cross-sectional SEM will be used to look at the film structure and electrical measurements such as four probe resistivity and Hall measurements may be employed. After deposition of the alternative buffer layer by chemical bath deposition (CBD), we will likely be able to deposit our own TCO and make a device out of each absorber.

4 Progress on the Epitaxial Growth of CuInSe2 Absorber Films

Participants: Timothy J. Anderson (Faculty Advisor), and Seokhyun Yoon

4.1 Objectives

Growth of epitaxial $CuInSe_2$ films with different Cu to In ratio and the study of their defect structure and the electrical properties.

4.2 Accomplishments during the current quarter

In earlier progress report, the existence of Cu-Se secondary phase was proposed in the Cu-rich CIS film, CIS3, from the compositional analysis and SEM analysis before and after KCN etching. It was also proposed that Cu-Se phase might exist on the surface of the film as the morphology of the film didn't change after etching. To further understand the growth habit of CIS on GaAs, cross-sectional TEM was used to view the morphology and the crystal structure of sample CIS3 coated with Pt. Transmission electron microscopy-Energy dispersive X-ray spectroscopy (TEM-EDX) was also used to determine the location of Cu-Se secondary phase. Dark field images of the island and matrix regions are shown in Figure 4-1. An island region consists of several large grains separated by gaps covered with a Cu-Se compound. To identify the location of Cu-Se secondary phase, TEM-EDX line-scans were taken for areas "A" and "B" in an island region and areas "C" and "D" in a matrix region as designated in Figure 4-1. The TEM-EDX depth profile of region A in the island region is shown in Figure 4-2. It shows Cu signal is very high near the surface of the island region, while the signals for other elements remained constant along the depth. This "Cu-rich phase" extends only about 10 nm from the surface. Figure 4-3 also shows the dark field image of near-surface region of the matrix and its TEX-EDX depth profile. It is shown in Figure 4-3 that matrix region is also covered with highly Cu-rich phase, which extends about 50 nm in this case. TEM-EDX depth profile analyses were also done for region "B" and region "D". They showed the same high Cu signal near the surface. The composition of the gap between the grains in island region "E" in Figure 4-1 (a) was also checked by TEM-EDX analysis. However, it didn't show high Cu signal. From these EDX results, it is concluded that Cu-Se secondary phase mainly exists on the surface of island region and the matrix region. It is also observed from the orientation of the matrix region in Figure 4-3(a) that the orientation of the matrix surface undulation is close to (112) crystal plane of $CuInSe_2$ as reported by D. Liao et. al.[1]. It was also reported that [112] plane of $CuInSe_2$ is stable and spontaneous decomposition of (220)/(204) surfaces to (112) facets by the first-principles calculation [2].

4.3 Activities envisioned for the next quarter

The cross-section of CIS films grown at higher temperature will be analyzed by TEM to study the crystal structure of CIS film grown on GaAs. TEM-EDX line scan will also be performed to identify the Cu-Se secondary phase and the possible Ga diffusion from the

substrate. Low temperature photoluminescence study and Hall measurement will also be performed on both samples to see the shallow defects in that film and their relation to the electrical transport properties.

4.4 References

[1] D. Liao and A. Rockett, "Epitaxial growth of Cu(In,Ga)Se_2 on GaAs (110)", *Journal of Applied Physics*, Vol. 91, pp. 1978-1983 (2002).

[2] S.B. Zhang and S.H. Wei, "Reconstruction and energetics of the polar (112) and (-1-1-2) versus the nonpolar (220)", *Physical Review B*, Vol. 65, pp. 081402-1-081402-4 (2002).

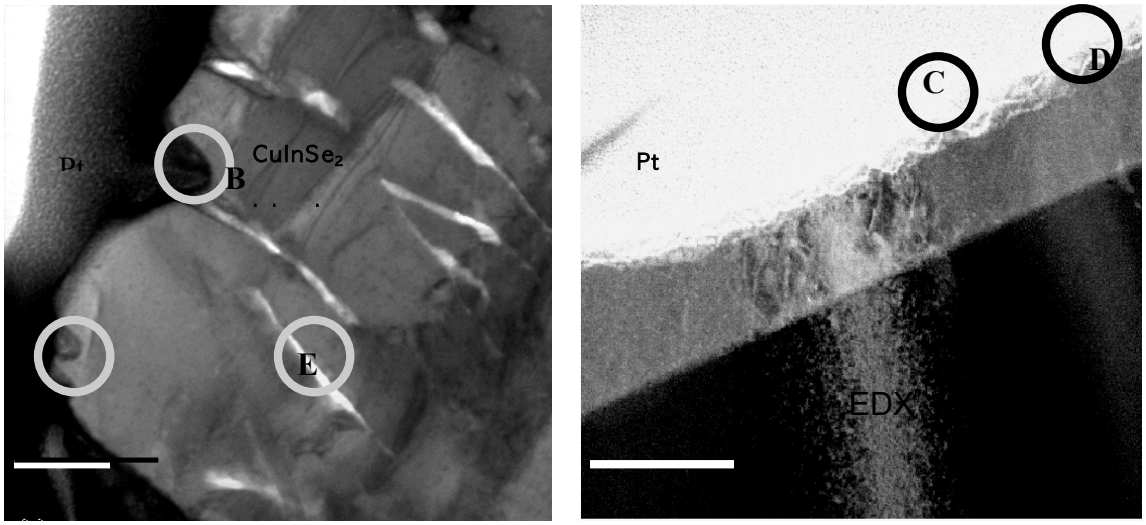

(a) Dark field image of an island region (b) Dark field image of a matrix region

Figure 4-1. TEM cross-sectional images of the Cu-rich sample Cu/In=1.09 (CIS3)

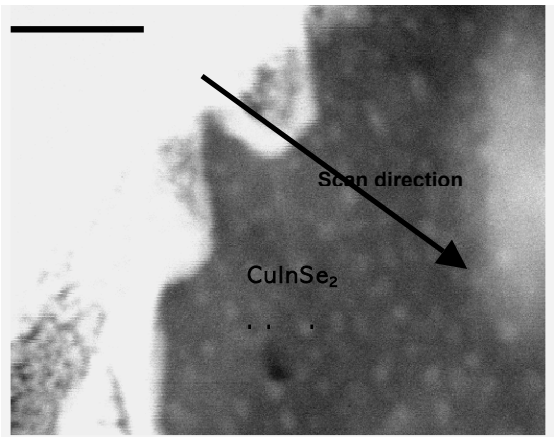

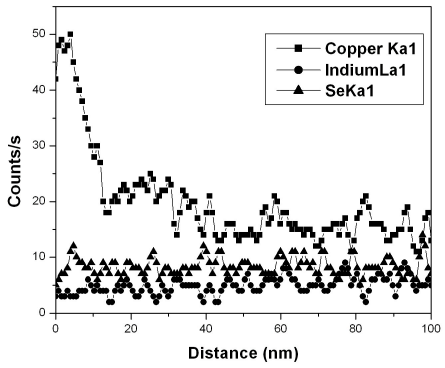

(a) Dark field image of EDX scan in region A

(b) EDX line scan of region A

Figure 4-2. TEM-EDX depth profile of an island region for the Cu-rich sample Cu/In=1.09 (CIS3)

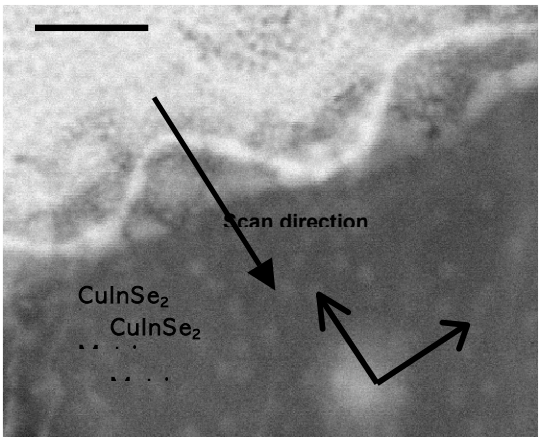

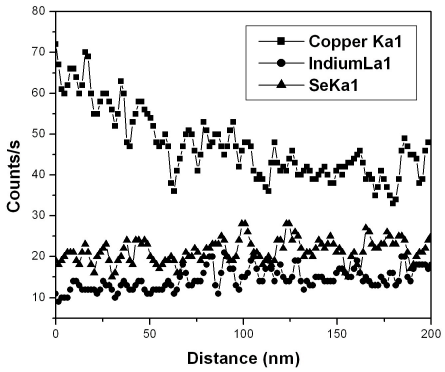

(a) Dark field image of TEM EDX scan region C

(b) EDX line scan of region C

Figure 4-3. TEM-EDX depth profile of matrix region :

Cu-rich sample Cu/In=1.09 (CIS3)

5 Progress on Development of Alternative Buffer Layers

Participants: Sheng S. Li (Faculty Advisor), and Jiyon Song and Seokhyun Yoon (Graduate Research Assistants).

5.1 Objectives

The objectives of this research task are to develop and optimize the chemical-bath-deposited (CBD) CdS and Cd-free alternative buffer layers for CIGS-based solar cells.

5.2 Accomplishments during the current quarter

During the current reporting period, we have focused our efforts on characterizing the as-deposited CBD-$Zn_xCd_{1-x}S$ thin films on the soda-lime glass (SLG) substrates by SEM and spectrophotometer to analyze the surface morphology and optical transmission spectral characteristics. The films with Zn composition of x = 0.3 and 0.5 demonstrated more than 70 % transmittance at wavelength longer than 600 nm.

The chemicals used in the work consist of aqueous solutions of 1.20×10^{-3} M $CdCl_2\cdot2(1/2)H_2O$, 1.39×10^{-3} M NH_4Cl, 1.19×10^{-2} M thiourea, 6.27×10^{-4} M $ZnCl_2$, and 5.27×10^{-4} M NH_3. The bath temperature was maintained between 80 and 85 °C. The deposition time ranged from 20 to 90 min. according to the mixture ratio of $[ZnCl_2]/([CdCl_2]+[ZnCl_2])$ in the solution. The film thickness and optical transmittance spectra of $Zn_xCd_{1-x}S$ films were measured by Tencor Profiler and HP 8453 UV-Visible spectrophotometer, respectively.

As shown in Figure 5-1, the film surface consists of wider grains as Zn content in the film increases. The thickness of the $Zn_xCd_{1-x}S$ films examined is in the range of 60 to 80 nm. Figure 5-2 shows the thickness variation with deposition time for $Zn_xCd_{1-x}S$ films with x = 0.3 and 0.5. The deposition rate decreases with increasing x. The films showed poor adherence, and colors varied from yellow to white-yellowish, as the composition of x increases up to 0.7. Similar behaviors have also been observed for the $Zn_xCd_{1-x}S$ films [1]. Figure 5-3 shows the optical transmittance spectra for $Zn_xCd_{1-x}S$ films with two Zn content values of x = 0.3 and 0.5. The spectral behavior of these films demonstrates that the absorption edges shift to shorter wavelengths with the increase of Zn content in the bath from 0.3 to 0.5. The thickness of these $Zn_xCd_{1-x}S$ films is measured in the range of 60 to 80 nm. The films have more than 70 % transmittance at wavelengths longer than 600 nm. These values are comparable with the reported values for $Zn_xCd_{1-x}S$ films reported elsewhere [2]. The spectral dependence of the transmittance for the $Zn_{0.3}Cd_{0.7}S$ film was measured, and the results are shown in Figure 5-4. For very thin $Zn_{0.3}Cd_{0.7}S$ films, better than 80 % transmittance were obtained at shorter and longer wavelengths, while film with thickness of 80 nm has a 70 % transmittance at wavelength longer than 600 nm.

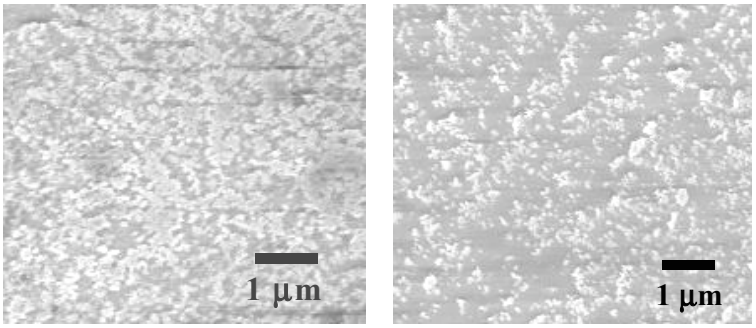

Zn 30 % 60 min. Zn 50 % 80 min.

Figure 5-1. SEM photographs of $Zn_xCd_{1-x}S$ films with x = 0.3 and 0.5 in the range of deposition time 60-80 min.

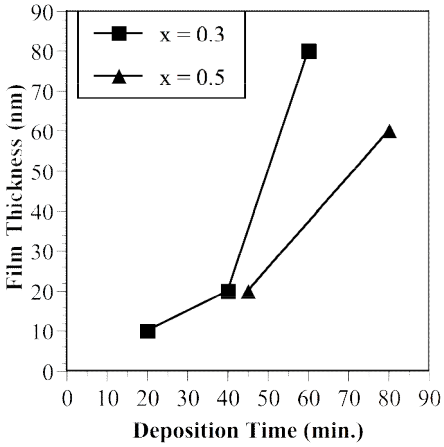

Figure 5-2. Film thickness variation as a function of deposition time for $Zn_xCd_{1-x}S$ films with x = 0.3 and 0.5.

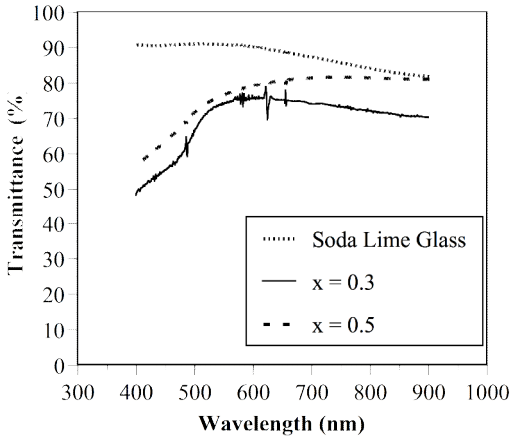

Figure 5-3. Optical transmittance spectra as a function of wavelength for $Zn_xCd_{1-x}S$ films with x = 0.3 and 0.5.

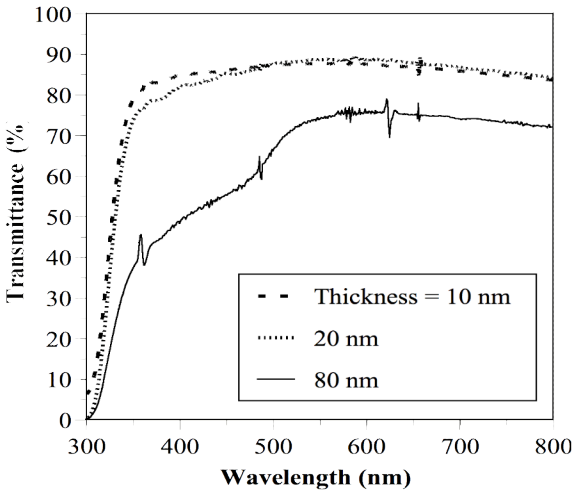

Figure 5-4. Optical transmittance spectra as a function of wavelength for $Zn_xCd_{1-x}S$ films with x = 0.3.

5.3 Activities envisioned for the next quarter

Our efforts for CIGS-based solar cells with alternative buffer layer of $Zn_xCd_{1-x}S$ will focus on optimizing CBD and annealing and conditions. Furthermore, the buffer layers of CdS and $Zn_xCd_{1-x}S$ will be deposited on the CIGS and CGS absorbers to investigate and compare the effect of different Zn composition of x on the performance of CIGS-based and CGS solar cells.

5.4 Publications and presentations

1. Jiyon Song, Sheng S. Li, S. Yoon, Jihyun Kim, W. K. Kim, T. J. Anderson, O. D. Crisalle, and Fan Ren, "Growth and Characterization of $Zn_xCd_{(1-x)}S$ Thin Film Buffer Layers by Chemical Bath Deposition", *Submitted in the 31st IEEE Photovoltaic Specialists Conference*, Lake Buena Vista, Florida, January 3-7 (2005).

2. Jiyon Song, Sheng S. Li, S. Yoon, T. J. Anderson, and O. D. Crisalle, "Growth and Characterization of $Zn_xCd_{1-x}S$ Buffer Layers by Chemical Bath Deposition for $CuGaSe_2$ and $Cu(In,Ga)Se_2$ solar cells", *Submitted in the Solar Energy Technologies Program Review Meeting*, Denver, Colorado, October 25-28 (2004).

5.5 References cited

[1] J. M. Dona and J. Herrero, "Chemical Bath Codeposited CdS-ZnS Film Characterization", *Thin Solid Films*, Vol. 268, pp. 5-12 (1995).

[2] T. Yamaguchi, Y. Yamamoto, T. Tanaka, Y. Demizu, and A. Yoshida, "(Cd,Zn)S Thin Films Prepared by Chemical Bath Deposition for Photovoltaic Devices", *Thin Solid Films*, Vol. 281-282, pp. 375-378 (1996).

6 Progress on Development of ZnO Sputtering

Participants: Oscar D. Crisalle (Faculty Advisor), and Wei Liu(Graduate Research Assistants) .

6.1 Objectives

The objective of ZnO sputtering is to deposit the transparent contact on top of buffer layer to make a further step toward a complete device. The target is to lower the resistivity of the ZnO film while maintaining a reasonable transmission in the visible range. The experiments are designed to find the optimum operating conditions to balance between the resistivity(and transmission.

6.2 Accomplishments during the current quarter

Non-reactive (pure Ar) sputtering was first attempted during this period and films with very low resistivity(in the range of 10^{-5} _-cm) was obtained but the transmission was very poor because the film was metal rich and oxygen deficient. SEM analysis was done to look at the surface structure and EDS was used to have a rough idea of the Zn and Oxygen ratio of these films. EDS analysis shows these films are Zn rich.

Then quasi-reactive sputtering (Ar and O_2 mixture sputtering) was later used to enhance oxygen concentration and hence improve the transmission. The transmission was improved significantly but as expected, the resistivity increases quickly.

Target treatment with an Ar and oxygen mixture was also attempted and non-reactive sputtering was used after the treatment. It was found that if the sputtering conditions are controlled in a certain region, non-reactive sputtering after target treatment can also yield highly transparent films. It was also noticed that by changing the sputtering conditions, the transmission can be manipulated. It was also found that under certain working pressure, if the deposition power goes beyond a value, the films become metal rich again and target treatment is required to regain transparent films.

6.3 Activities envisioned for the next quarter

Concentrate on the non-reactive sputtering after target treatment and optimize the sputtering conditions to lower the resistivity. Maintain the average transmission in the visible range above 80% to make it viable for solar cell applications. Optimize the ZnO film thickness to further lower the resistivity if it is possible. Necessary characterization will be done to help analyze the films.